nature cell biology

Tension applied through the Dam1 complex promotes microtubule elongation providing a direct mechanism for length control in mitosis

Andrew D. Franck[1,3], Andrew F. Powers[1,3], Daniel R. Gestaut[2], Tamir Gonen[2], Trisha N. Davis[2] and Charles L. Asbury[1,4]

In dividing cells, kinetochores couple chromosomes to the tips of growing and shortening microtubule fibres[1,2] and tension at the kinetochore–microtubule interface promotes fibre elongation[3–6]. Tension-dependent microtubule fibre elongation is thought to be essential for coordinating chromosome alignment and separation[1,3,7–10], but the mechanism underlying this effect is unknown. Using optical tweezers, we applied tension to a model of the kinetochore–microtubule interface composed of the yeast Dam1 complex[11–13] bound to individual dynamic microtubule tips[14]. Higher tension decreased the likelihood that growing tips would begin to shorten, slowed shortening, and increased the likelihood that shortening tips would resume growth. These effects are similar to the effects of tension on kinetochore-attached microtubule fibres in many cell types, suggesting that we have reconstituted a direct mechanism for microtubule-length control in mitosis.

For decades, a central problem for biologists has been to understand how microtubule lengths are controlled during mitosis[15,16]. Microtubules are protein polymers that switch stochastically between phases of assembly and disassembly, during which tubulin subunits are added or lost from the filament tips[1]. This behaviour, called dynamic instability, can be described by four parameters: the speeds of growth and shortening, and the rates of switching from growth to shortening and from shortening to growth — transitions known as catastrophes and rescues[1,17]. In dividing cells, chromosomes are linked to the tips of microtubule fibres through specialized structures called kinetochores, and their movements are coupled to fibre growth and shortening[1,2]. Remarkably, kinetochores maintain persistent, load-bearing attachments to microtubule tips even as the filaments assemble and disassemble under their grip[1,2,18]. Classic micromanipulation experiments show that tension at the kinetochore–microtubule interface promotes microtubule fibre elongation[3–6], and this effect is widely believed to be essential for controlling fibre lengths and thereby coordinating chromosome alignment and separation[1,3,7–10,16]. Very little is known about the mechanism underlying this tension-dependent length control. However, the dynamic behaviour of kinetochore-attached microtubule tips[18] implies that the mechanism underlying tension-dependent length control *in vivo* may act by altering one or more of the parameters of dynamic instability in response to load.

A key unanswered question is whether tension promotes elongation through an indirect mechanism, where force transmitted through load-bearing kinetochore components regulates the activity of separate microtubule-modifying components, or by a direct mechanism, where the load-bearing components themselves modulate microtubule behaviour. Indirect regulation through microtubule-modifying enzymes has been implicated in corrective detachment of aberrant kinetochore–microtubule attachments[19–21], but it is unknown whether an analogous indirect mechanism also controls the lengths of microtubules that remain persistently attached. Evidence for a simpler direct mechanism comes from cell-free assays showing that compressive force caused by pushing microtubule tips against glass barriers slows filament growth[22,23], and that brief pulses of tension <1 pN transmitted through avidin–biotin linkages can delay detachment of terminal subunits[24]. However, these approaches do not allow measurement of microtubule dynamic parameters under continuous tension, thus their relevance to length control of kinetochore microtubules, which are usually under tension[5,25], is uncertain.

To overcome these limitations, we relied on a motility assay using the Dam1 complex[11] (also known as DASH, or DDD), a putative load-bearing component of kinetochores in yeast[11–14,26]. Similarly to kinetochores, pure recombinant Dam1 complex forms robust connections to growing and shortening microtubule tips that remain attached even when tension is applied[14]. This persistent tip tracking has enabled measurement of the effects of continuous tension on microtubule dynamic parameters in a reconstituted system for the first time. In our assay, beads coated with the Dam1 complex are attached to the

[1]Departments of Physiology & Biophysics, University of Washington, Seattle, WA 98195, USA. [2]Department of Biochemistry, University of Washington, Seattle, WA 98195, USA. [3]These authors contributed equally to this work.
[4]Correspondence should be addressed to C.L.A. (e-mail: casbury@u.washington.edu)

Received 15 February 2007; accepted 24 May 2007; published online 17 June 2007; DOI: 10.1038/ncb1609

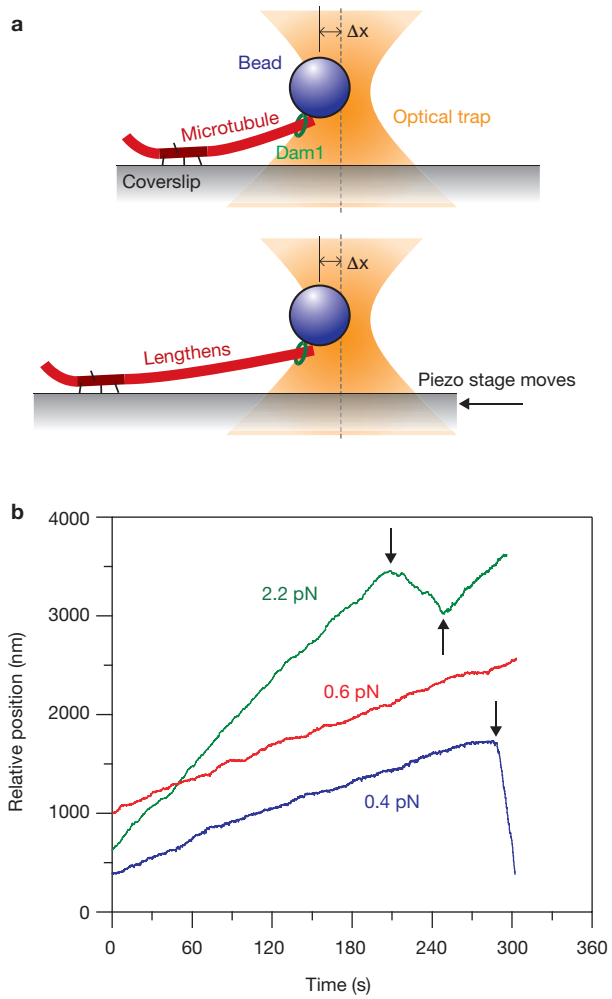

Figure 1 Recording microtubule dynamics with tension applied by an optical trapping-based force clamp. (**a**) Schematic representation showing experimental geometry and force-clamp operation. A polystyrene bead (blue) is held by an optical trap (orange). The Dam1 complex (green) on the bead surface mediates attachment to the tip of a dynamic microtubule (red). A portion of the microtubule (dark red) is anchored to the coverslip. As the microtubule grows and shortens, the coverslip is moved by computer to keep a fixed separation (Δx) between the bead and trap, thereby maintaining a constant level of tension. (**b**) Three (of $n = 298$) representative records showing position against time for tip-attached beads under tension. Increasing position represents bead movement away from the anchored portion of the filament during microtubule growth. Decreasing position represents movement toward the anchored seed during filament shortening. Arrows mark catastrophe and rescue events. More example records are shown in Fig. 2.

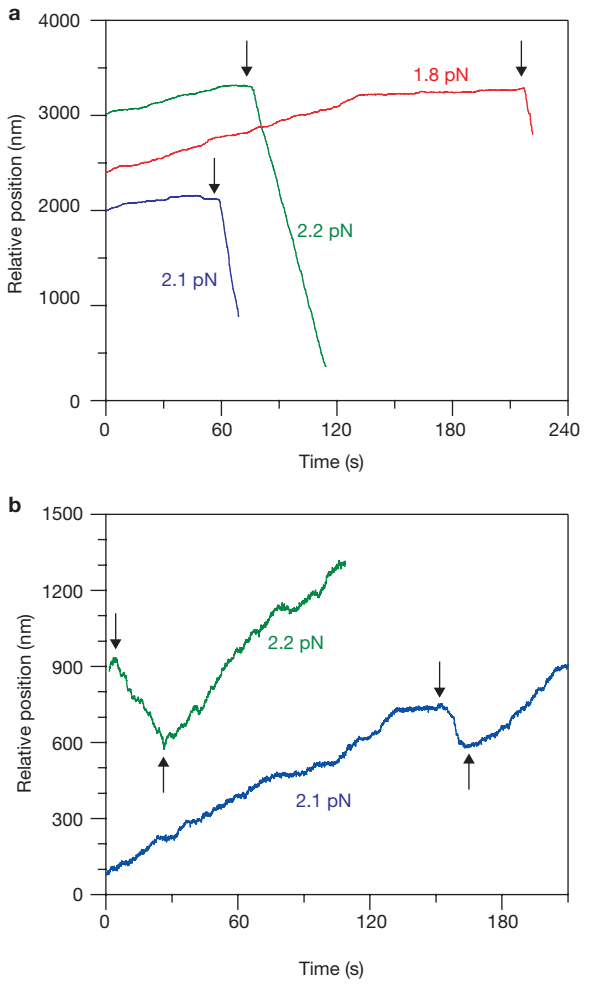

Figure 2 Additional records showing microtubule dynamics with applied tension. (**a**) Three records showing growth, catastrophe (arrows), and shortening at the indicated levels of tension. (**b**) Two records showing growth, catastrophe (downward arrows), shortening and rescue (upward arrows).

tips of individual dynamic microtubules grown from stabilized seeds anchored to a glass coverslip[14,22,23] (Fig. 1a). Tension is applied to the filament tip using an optical trapping-based force clamp that moves the specimen stage under feedback control[14]. Changes in microtubule length are accommodated while keeping a fixed offset between the tip-attached bead and the centre of the optical trap, thus maintaining a constant tensile force. Microtubule growth and shortening is recorded by monitoring the position of the stage.

When a Dam1-coated bead was attached to a growing microtubule tip and placed under tension, it moved slowly away from the coverslip-anchored seed as the intervening portion of the filament lengthened (840 ± 80 nm on average, $n = 298$ records). Sometimes the bead detached from the growing microtubule (Fig. 1b, red trace). However, as reported previously[14], it sometimes remained attached long enough for the filament to undergo catastrophe. After catastrophe, the shortening microtubule carried the bead back toward the seed (1400 ± 330 nm, $n = 72$), performing work against the tension applied by the optical trap (Figs 1b and 2, and see Supplementary Information, Movie S1). To allow frequent catastrophes to be observed, we operated at relatively low tubulin concentration (9–12 μM). Under these conditions, the filament usually disassembled completely back to the seed after catastrophe and the bead usually detached during shortening. However, occasionally the filament was rescued and the bead resumed assembly-coupled movement (Figs 1b and 2b, and see Supplementary Information, Movie S2). These observations show that growth, shortening, catastrophe and rescue can all be recorded with continuous tension using our Dam1-based motility assay.

To determine whether microtubule dynamic parameters are sensitive to tension, the movement of tip-attached beads was recorded at two levels of force, either 0.5 ± 0.2 pN or 2.0 ± 0.2 pN (Fig. 3 and Table 1). Growth and shortening speeds were obtained for each record by plotting traces of position over time and fitting lines to the appropriate

Table 1 Microtubule-dynamic parameters measured at different levels of tension

Tensile force (pN)	0.5 ± 0.2	2.0 ± 0.2
Number of growth events	87	211
Mean growth speed (nm s^{-1})	6.0 ± 0.8	5.8 ± 0.3
Total growth time (h)	4.594	7.888
Number of catastrophes	44	28
Catastrophe frequency (h^{-1})	9.6 ± 1.4	3.5 ± 0.7
Detachments during growth	27	149
Detachments frequency (h^{-1})	5.9 ± 1.1	19 ± 2
Number of shortening events	44	28
Mean shortening speed (nm s^{-1})	158 ± 26	56 ± 10
Total shortening time (h)	0.212	0.068
Number of rescues	3	7
Rescue frequency (h^{-1})	14 ± 8	103 ± 39
Detachments during shortening	32	20
Detachment frequency (h^{-1})	150 ± 30	290 ± 70

segments. The distributions of growth speed were very similar at the two levels of force (Fig. 3a), with mean values consistent with previous *in vitro* measurements[17]. The mean growth speed at 0.5 pN was 6.0 ± 0.8 nm s^{-1}, not significantly different ($P = 0.42$) from the mean speed at 2.0 pN, which was 5.8 ± 0.3 nm s^{-1} (Fig. 3c). The insensitivity of growth speed to tension indicates that the effective binding rate of free tubulin to the microtubule tip is load-independent under the conditions of our assay. In contrast, the distribution of microtubule shortening speeds at 2.0 pN was shifted towards lower values compared to 0.5 pN (Fig. 3b). The mean shortening speed at 2 pN was 56 ± 10 nm s^{-1}, which was significantly slower ($P = 0.00022$) than the mean speed at 0.5 pN, which was 158 ± 26 nm s^{-1} (Fig. 3d). The observation that, on average, filaments under higher tension shorten more slowly suggests that microtubule disassembly is sensitive to tension.

If the effect of tension on disassembly is direct, then abrupt changes in the level of tension should cause immediate changes in shortening speed. To test this hypothesis, we programmed our force clamp to automatically switch the level of tension during episodes of microtubule disassembly. After a specified amount of shortening occurred at the initial tension, the force was either increased (Fig. 4a, c) or decreased (Fig. 4b). Switching the force required ~0.2 s, during which elastic elements (for example, seed-coverslip linkage, Dam1-bead linkage, etc.) stretched or relaxed depending on whether the force was increased or decreased. Thereafter, disassembly continued at the new, constant level of force. Fig. 4c shows an example where the force was increased from 0.5 to 2.0 pN, causing an immediate reduction in shortening speed, from 100 to 63 nm s^{-1}, which persisted >25 s before bead detachment. Fig. 4b shows an example where the force was decreased from 1.9 to 0.3 pN, and the speed increased from 104 to 322 nm s^{-1}. To estimate the sensitivity of shortening speed to force, many records ($n = 27$) were collected where the force was switched between 0.5 ± 0.2 and 2.0 ± 0.2 pN. For each record, the sensitivity was quantified by computing $\Delta speed\ \Delta force^{-1}$ — the change in shortening speed divided by the change in tension. The distribution of sensitivity values was broad, with a mean sensitivity of –40 ± 7 nm s^{-1} pN^{-1} (Fig. 4c). This average agrees well with the mean sensitivity estimated from our prior measurements at constant force, which was –68 ± 28 nm s^{-1} pN^{-1} (Fig. 3d and Table 1), and indicates that shortening speeds are reduced when tension is increased. The observation that force can cause an immediate and persistent change in shortening speed confirms that tension affects microtubule disassembly in a direct manner.

Microtubule-length distributions are exquisitely sensitive to catastrophe and rescue frequencies[27–29], therefore we wanted to determine whether these switching rates are also altered by changes in tension. To estimate catastrophe and rescue rates, the number of switching events observed under constant force was counted and divided by the total observation time. At 0.5 pN, 44 catastrophes were recorded during 87 episodes of microtubule growth, with a combined duration of 4.594 h. On this basis, a catastrophe frequency of 9.6 ± 1.4 h^{-1} was estimated (Table 1). At 2.0 pN, 28 catastrophes were recorded during 211 growth episodes lasting 7.888 h, giving a catastrophe frequency of 3.5 ± 0.7 h^{-1}, which was significantly lower ($P = 0.00008$) than at 0.5 pN (Fig. 3e). Rescues were comparatively rare in our experiments, partly due to frequent bead detachment during disassembly (Fig. 3h). Nevertheless, seven rescue events were recorded in 0.068 h of shortening at 2.0 pN, whereas at 0.5 pN only three events were recorded in 0.212 h (Table 1). From these observations, a rescue frequency of 14 ± 8 per h was calculated at 0.5 pN, and a sevenfold higher frequency of 103 ± 39 per h was calculated at 2.0 pN ($P = 0.013$, Fig. 3f).

The lower catastrophe and higher rescue frequencies at 2 pN imply that, for a population of microtubules, the proportion of time spent in the growth phase increases as tension increases. The lower shortening speed will also reduce the extent of disassembly during episodes of shortening. Numerous other studies have shown that similar changes, particularly reductions in the catastrophe frequency, dramatically promote microtubule elongation[27–29]. Depending on switching frequencies and growth and shortening speeds, a population of microtubules polymerized from stable seeds can exhibit two very different classes of behaviour: steady state, where the average microtubule length reaches a constant value; and unbounded growth, where the population grows indefinitely (until the free tubulin is depleted)[29]. The rate parameters that were measured at 0.5 pN are consistent with the steady-state scenario, with an average length of 2400 ± 500 nm. In contrast, the rates at 2.0 pN are consistent with unbounded growth, with an average length for the population that increases by 3.7 ± 1.0 nm s^{-1}. These population-average values are calculated from the measured growth, shortening, catastrophe, and rescue rates, as described in the Methods. In light of these considerations, our observations indicate that the microtubules in our assay are strongly biased toward elongation at higher levels of tension.

The tension-dependent behaviour that was observed here with Dam1 and individual microtubules is strikingly similar to the behaviour of kinetochores and their attached microtubule fibres in a wide variety of cells[3–6,9,30]. For example, tugging on chromosomes in grasshopper spermatocytes using microneedles causes the kinetochore-attached fibres opposing the load to lengthen[3], consistent with our central conclusion that tension promotes net microtubule elongation. Likewise, our observation that tension inhibits catastrophe and promotes rescue is consistent with observations of kinetochore 'directional instability' in PtK_1 and newt lung cells[4–6,9,30], where increased tension causes kinetochore-attached fibres to switch from shortening to growth[4], and loss of tension causes switching from growth to shortening[4–6]. These similarities suggest that tension at kinetochore–microtubule interfaces *in vivo* modulates the dynamics of attached microtubules in a direct manner analogous to our *in vitro* experiments. We note, however, that an alternative explanation for the above-mentioned experiments with animal cells,

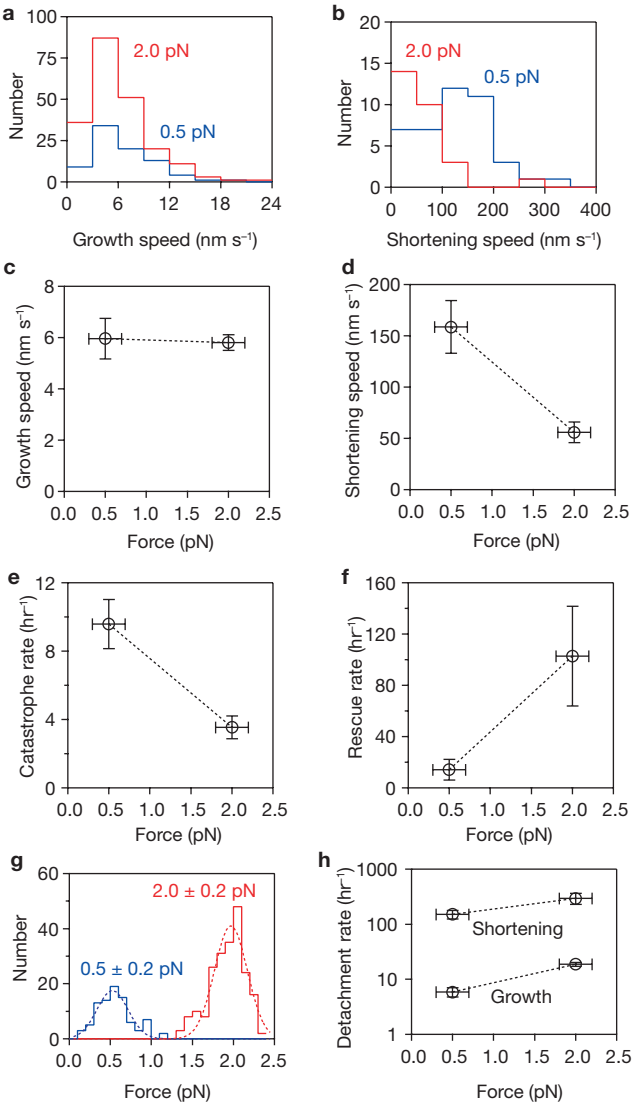

Figure 3 Tension slows shortening, inhibits catastrophe and promotes rescue. (**a**, **b**) Distributions of growth and shortening speeds at two levels of tension. Growth speed distributions at 2.0 pN (**a**, red) and 0.5 pN (**a**, blue) are similar in shape. The distribution of shortening speeds, however, is shifted toward lower values at 2.0 pN (**b**, red) compared to 0.5 pN (**b**, blue). (**c**, **d**) Mean growth (**c**) and shortening speeds (**d**) plotted against tensile force. Uncertainties in speed and force represent s.e.m. and s.d., respectively (n values are shown in Table 1). (**e**, **f**) Catastrophe (**e**) and rescue (**f**) rates plotted against tensile force. Uncertainties in transition rates represent counting errors (n values are shown in Table 1). (**g**) Distributions of tensile force for the dataset. (**h**) Rates of bead detachment from shortening and growing tips, estimated by counting the number of detachment events and dividing by the total observation time in each phase. Uncertainties in detachment rate represent counting errors (n values are shown in Table 1).

in which each kinetochore binds multiple microtubules, is theoretically possible[31]. Kinetochore directional switching could occur without tension-dependent changes in microtubule dynamic rates if shortening filaments under high tension detach and are subsequently replaced by new, growing filaments. But this detachment-driven mechanism is untenable in budding yeast, where each kinetochore binds a single microtubule tip[32] and tension-dependent control of microtubule dynamics is strongly implicated[8,32]. Our experiments show that such control can be exerted directly, through the Dam1 complex or other load-bearing kinetochore components, perhaps acting in concert with indirect mechanisms mediated by additional microtubule-modifying agents.

It is instructive to compare our results with previous measurements of microtubule dynamics under compressive force. Microtubule tips growing against rigid barriers can generate a few pN of compressive force, which is enough to reduce their growth speed approximately threefold[22,33] and to promote catastrophe[23]. The catastrophe frequency in such experiments scales with the reciprocal of growth speed over a range of tubulin concentrations independently of whether compressive force is applied, suggesting that compression promotes catastrophe only by limiting the rate of tubulin addition[23]. This relatively simple interpretation, however, cannot explain our results. Whereas forces of similar magnitude are sufficient to alter microtubule dynamics in either experiment (2 pN of tension versus 2–4 pN of compression[22,33]), the net effect of tension in our assay is to promote microtubule growth by altering filament behaviour, including the catastrophe frequency, without significantly changing the speed of growth. This difference suggests that the two methods of applying force differ not only in the direction of force, but also in the underlying mechanism by which force alters microtubule dynamics.

Understanding the structural basis for coupling between the Dam1 complex and microtubule tips is of great interest, and it is critical for understanding mechanistically how tension transmitted through the complex affects filament dynamics. The data presented here provide some clues about the nature of this interaction, but considerable uncertainty remains. The tips of shortening microtubules are frayed because individual rows of tubulin subunits, called protofilaments, curl outward and peel away from the main filament before breaking off[34]. The Dam1 complex may transmit tension to these outwardly curling protofilaments, tending to straighten them. Disassembly would be slowed in this interpretation because the protofilaments must overcome the tension as they peel away from the main filament. The same scenario could explain how tension affects catastrophe and rescue frequencies, as these transitions may also involve protofilament curling and straightening, respectively. The ring model proposed recently for Dam1-based coupling to microtubule tips[12–14,26] is consistent with this hypothesis. When pure recombinant Dam1 complex is mixed with stabilized microtubules it oligomerizes into rings encircling the filaments[12,13]. To drive movement, peeling protofilaments may act as a 'conformational wave'[2] that propagates in the direction of shortening, and pushes continuously against a ring of Dam1 and also against any external tension applied to the ring. We have confirmed that under the buffer conditions of our experiments, free Dam1 complex (that is, not bead bound) is capable of forming rings (see Supplementary Information, Fig. S1). Additional experiments will be required to determine whether the bead-bound Dam1 complex in our assays can also form rings and, if so, whether they are necessary for the tension-dependent effects reported here.

Tension-induced microtubule elongation is widely believed to be essential for controlling mitotic chromosome movements in organisms as diverse as yeast[8,32], insects[3,7,10] and vertebrates[6,9]. Our work demonstrates that this effect can be reconstituted in a simple system. The effect is direct, in the sense that pure recombinant Dam1 complex without additional factors is sufficient to form load bearing attachments that also modify microtubule dynamics in response to the load. Important questions remain about the underlying mechanism, particularly regarding the structure of Dam1-based microtubule attachments. Regardless of the

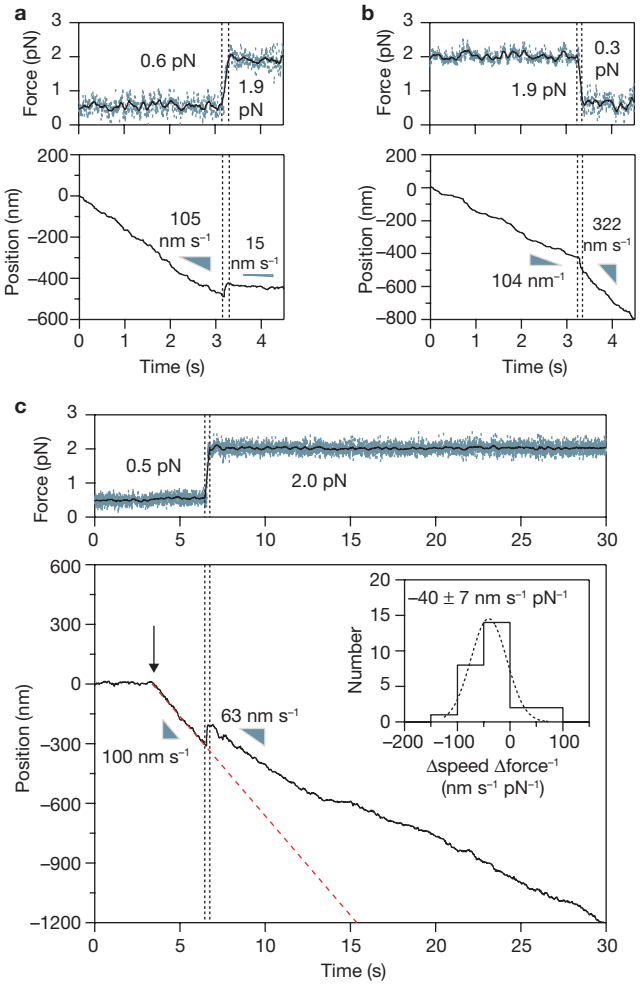

Figure 4 Changing the level of tension during movement immediately alters shortening speed. (**a**–**c**) Three (of $n = 27$) representative records showing tensile force (upper plots) and bead position (lower plots) against time during disassembly-driven movement. In these force-switch experiments, the instrument was programmed to automatically change the level of tension after a pre-specified amount of movement occurred. Dashed vertical lines denote intervals (~0.2 s duration) when the force was changing. Shortening speeds before and after the change in force are indicated (grey triangles). In **c**, the arrow marks a catastrophe and the dashed red line shows a least-squares fit to the portion of the trace preceding the change in force. The inset shows the distribution of sensitivities, $\Delta speed\ \Delta force^{-1}$, computed from each record by dividing the change in speed by the change in force.

structural basis, however, our finding that a load-bearing kinetochore component alters filament dynamics in a tension-dependent manner suggests a general mechanism for microtubule length control *in vivo*. In principle, such a mechanism could operate wherever dynamic microtubules form tension-bearing tip attachments, for example, at kinetochores, spindle poles and the cell cortex. □

METHODS

Protein purification. All ten subunits of the Dam1 complex were expressed in *Escherichia coli* (BL21 Rosetta; Novagen, Madison, WI) from a single plasmid (gift from J. J. Miranda and S. C. Harrison, Harvard University, Boston, MA) and purified essentially as previously described[12–14]. The gene for one subunit (Spc34p) included a His6x-tag to facilitate purification and bead binding. Cells harbouring the plasmid were induced to express the complex in mid-log phase by addition of 0.2 mM IPTG, grown for 5 h at 37 °C, pelleted and snap frozen. Pellets were resuspended in phosphate buffer (20 mM phosphate at pH 7.0, 500 mM NaCl, 1 mM PMSF and complete protease inhibitors without EDTA from Roche, Indianapolis, IN), lysed in a French press and clarified by centrifugation. The supernatant was mixed with metal-affinity resin (Talon; BD Biosciences, San Jose, CA), washed in phosphate buffer, and eluted with 200 mM imidazole. The eluate was purified on a size-exclusion column (Superdex 200 10/300GL; Amersham Biosciences, Piscataway, NJ), equilibrated with phosphate buffer, and snap frozen in phosphate buffer plus 10% glycerol.

Motility assays. To bind the His6x-tagged complex, 0.44-μm-diameter streptavidin-coated polystyrene beads (Spherotech, Lake Forest, IL) were further functionalized by incubation with biotinylated penta-His antibody (Qiagen, Valencia, CA) and washed in BRB80 (80 mM PIPES, 1 mM $MgCl_2$, 1 mM EGTA at pH 6.9) plus 8 mg ml^{-1} bovine serum albumin (BSA), included as a blocking protein. Dilute suspensions of anti-His beads (0.01% solids) were coated with Dam1 by mixing with 24 nM of the heterodecameric complex in BRB80 plus BSA and incubating for 90 min. Free Dam1 was then removed by centrifugation before introducing the beads into the flow chamber. Stable microtubule seeds were grown by incubating 68 μM bovine brain tubulin, 1 μM biotinylated tubulin (Cytoskeleton, Denver, CO) and 1 mM GMPCPP (Jena Bioscience, Jena, Germany) in BRB80 plus 10% glycerol at 37 °C for >30 min. KOH-cleaned coverslips were fixed with double-sided sticky tape to glass slides to create flow chambers, which were functionalized by incubation with 5 mg ml^{-1} biotinylated BSA (Vector Labs, Burlingame, CA) followed by 0.3 mg ml^{-1} avidin DN (Vector Labs). Seeds were bound and then washed with growth buffer (BRB80 plus BSA with 1 mM GTP) before introduction of Dam1 beads and 9–12 μM tubulin in growth buffer supplemented with 1 mM DTT and an oxygen scavenging system consisting of 250 μg ml^{-1} glucose oxidase, 30 μg ml^{-1} catalase and 4.5 mg ml^{-1} glucose. After microtubule growth, thermal fluctuations tended to bend the extensions slightly away from the coverslip, making them distinguishable from the seeds and making their tips accessible for bead binding. Beads were attached exclusively to microtubule plus ends, which were identified by their greater extension length compared to minus ends. The accuracy of this assignment was >98%, judging from control experiments in which kinesin-coated beads were used to determine unambiguously which end was the plus end (data not shown). We chose to work at low tubulin concentration to maximize the catastrophe frequency while still allowing microtubule extensions of sufficient length to grow from the coverslip-anchored seeds. The dataset shown in Table 1 and Fig. 3 was generated using two different preparations of tubulin. Because the fraction of active tubulin typically varies slightly between preparations[17,33], the relative concentrations were adjusted to match microtubule growth rates. With this adjustment, all microtubule dynamic parameters measured with applied tension for the two preparations were statistically indistinguishable, so the data were combined. Assays were performed at 22 °C.

Instrumentation and data collection. The optical trap was essentially as described previously[14]. Position-sensor response was mapped using the piezo stage to raster-scan a coverslip-attached bead through the beam, and trap stiffness was calibrated along the two principle axes using the drag force, equipartition and power spectrum methods. Feedback was implemented with custom LabView software. During clamping, bead-trap separation was sampled at 40 kHz while stage position was updated at 50 Hz to maintain the desired load. Bead and stage position data were decimated to 200 Hz before storing to disk. For experiments where force was changed during microtubule-driven movement, the instrument was programmed to automatically switch to the new level of tension after the bead travelled a user-specified distance in the direction of disassembly (typically 250–500 nm).

Data analysis. Periods of slow microtubule growth and rapid shortening were easily identified in the records of relative bead position versus time. Growth and shortening speeds were obtained from best-fit lines to portions of these records. For constant force experiments (Figs 1–3), shortening speeds were obtained from fits to the last half of the disassembly-driven movement to avoid brief periods of acceleration, usually lasting ~1 s, which sometimes occurred just after the onset of shortening. Catastrophes were scored and shortening speeds were recorded only when a bead moved in the direction of disassembly by an amount that clearly exceeded the level of random noise in the trace (that is, by >40 nm). Similarly, rescues were scored only when a clear episode of disassembly-driven movement

(>40 nm) was followed again by slow growth. For the force-switch experiments (Fig. 4), shortening speeds immediately before and after the change in tension were obtained by fitting 100 nm of movement on either side of the switch. Uncertainties reported for mean speeds represent s.e.m. and corresponding significance levels were estimated using both the one-tailed Student's *t*-distribution and the Kolmogorov-Smirnov test. Both methods yielded essentially the same results, so only *P* values from the *t*-tests are reported here. Uncertainties reported for catastrophe and rescue rates represent counting errors, computed as $\delta r = t^{-1}\sqrt{N}$ where t is the total observation time and N is the number of transition events. These uncertainties were used to calculate the corresponding significance levels, assuming normally distributed rates with standard deviations given by δr.

Two formulas from the literature were used to estimate how the tension-dependent changes in the microtubule-dynamic parameters measured would affect net length for a population of microtubules. Depending on parameter values, a microtubule population can exist in either a steady state regime, where the average length reaches a constant value, or an unbounded growth regime, where the population grows indefinitely (until the free tubulin is depleted)[29]. The first formula, adapted from ref. 29, represents the mean length, $\langle L \rangle$, for a population of microtubules in the steady state regime: $\langle L \rangle = v_s v_g (v_s f_c - v_g f_r)^{-1}$ The second formula, adapted from ref. 17, represents the mean rate of growth, $\langle J \rangle$, for a population in the unbounded growth regime: $\langle J \rangle = (v_g f_c^{-1} - v_s f_r^{-1})(f_c^{-1} + f_r^{-1})^{-1}$ Here, v_g and v_s are the growth and shortening speeds, and f_c and f_r are the catastrophe and rescue frequencies, respectively.

Electron microscopy. Dam1 complex was mixed with taxol-stabilized microtubules to final concentrations of 20 nM Dam1 and 80 nM tubulin in motility buffer (BRB80 supplemented with 8 mg ml^{-1} BSA, 1 mM GTP, 1 mM DTT, and an oxygen scavenging system consisting of 250 μg ml^{-1} glucose oxidase, 30 μg ml^{-1} catalase and 4.5 mg ml^{-1} glucose) plus 10 μM taxol, incubated 10 min, and fixed by addition of three volumes of 2% glutaraldehyde. Samples were then negatively stained and viewed on a transmission electron microscope, as follows. Carbon coated electron microscopy cupper grids (EMS) were positively charged on a plasma cleaner (EMS-100, EMS). A 4 μl droplet of each sample was pipetted onto a clean grid, washed with water and stained with 2% uranyl acetate in water. Grids were air-dried and viewed on a 120 kV JEM 1230. Images were recorded on a 2k × 2k Gatan slow-scan charge-coupled device camera.

Note: Supplementary Information is available on the Nature Cell Biology website.

ACKNOWLEDGEMENTS

We thank J. J. Miranda and S. C. Harrison (Harvard Medical School) for providing the expression plasmid for the Dam1 complex, and B. Graczyk for electron microscopy sample preparation. This work was supported by a Searle Scholar Award (to C.L.A.), and by grants from the National Institutes of Health (to T.N.D. and C.L.A.). A.F.P. was supported by a National Institutes of Health (NIH) training grant, T32 GM07270.

COMPETING FINANCIAL INTERESTS

The authors declare that they have no competing financial interests.

Published online at http://www.nature.com/naturecellbiology/
Reprints and permissions information is available online at http://npg.nature.com/reprintsandpermissions/

1. Inoue, S. & Salmon, E. D. Force generation by microtubule assembly/disassembly in mitosis and related movements. *Mol. Biol. Cell* **6,** 1619–1640 (1995).
2. Koshland, D. E., Mitchison, T. J. & Kirschner, M. W. Polewards chromosome movement driven by microtubule depolymerization *in vitro*. *Nature* **331,** 499–504 (1988).
3. Nicklas, R. B. The forces that move chromosomes in mitosis. *Annu. Rev. Biophys. Biophys. Chem.* **17,** 431–449 (1988).
4. Skibbens, R. V. & Salmon, E. D. Micromanipulation of chromosomes in mitotic vertebrate tissue cells: tension controls the state of kinetochore movement. *Exp. Cell Res.* **235,** 314–324 (1997).
5. Khodjakov, A. & Rieder, C. L. Kinetochores moving away from their associated pole do not exert a significant pushing force on the chromosome. *J. Cell Biol.* **135,** 315–327 (1996).
6. Skibbens, R. V., Rieder, C. L. & Salmon, E. D. Kinetochore motility after severing between sister centromeres using laser microsurgery: evidence that kinetochore directional instability and position is regulated by tension. *J. Cell Sci.* **108,** 2537–2548 (1995).
7. Goshima, G., Wollman, R., Stuurman, N., Scholey, J. M. & Vale, R. D. Length control of the metaphase spindle. *Curr. Biol.* **15,** 1979–1988 (2005).
8. Gardner, M. K. *et al*. Tension-dependent regulation of microtubule dynamics at kinetochores can explain metaphase congression in yeast. *Mol. Biol. Cell* **16,** 3764–3775 (2005).
9. Skibbens, R. V., Skeen, V. P. & Salmon, E. D. Directional instability of kinetochore motility during chromosome congression and segregation in mitotic newt lung cells: a push-pull mechanism. *J. Cell Biol.* **122,** 859–875 (1993).
10. Civelekoglu-Scholey, G., Sharp, D. J., Mogilner, A. & Scholey, J. M. Model of chromosome motility in *Drosophila* embryos: adaptation of a general mechanism for rapid mitosis. Biophys. J. **90,** 3966–3982 (2006).
11. Cheeseman, I. M., Drubin, D. G. & Barnes, G. Simple centromere, complex kinetochore: linking spindle microtubules and centromeric DNA in budding yeast. *J. Cell Biol.* **157,** 199–203 (2002).
12. Miranda, J. J., De Wulf, P., Sorger, P. K. & Harrison, S. C. The yeast DASH complex forms closed rings on microtubules. *Nature Struct. Mol. Biol.* **12,** 138–143 (2005).
13. Westermann, S. *et al*. Formation of a dynamic kinetochore- microtubule interface through assembly of the Dam1 ring complex. *Mol. Cell* **17,** 277–290 (2005).
14. Asbury, C. L., Gestaut, D. R., Powers, A. F., Franck, A. D. & Davis, T. N. The Dam1 kinetochore complex harnesses microtubule dynamics to produce force and movement. *Proc. Natl Acad. Sci. USA* **103,** 9873–9878 (2006).
15. Inoue, S. & Ritter, H., Jr. Dynamics of mitotic spindle organization and function. *Soc. Gen. Physiol. Ser.* **30,** 3–30 (1975).
16. Nicklas, R. B. Measurements of the force produced by the mitotic spindle in anaphase. *J. Cell Biol.* **97,** 542–548 (1983).
17. Walker, R. A. *et al*. Dynamic instability of individual microtubules analyzed by video light microscopy: rate constants and transition frequencies. *J. Cell Biol.* **107,** 1437–1448 (1988).
18. Maddox, P., Straight, A., Coughlin, P., Mitchison, T. J. & Salmon, E. D. Direct observation of microtubule dynamics at kinetochores in *Xenopus* extract spindles: implications for spindle mechanics. *J. Cell Biol.* **162,** 377–382 (2003).
19. Andrews, P. D. *et al*. Aurora B regulates MCAK at the mitotic centromere. *Dev. Cell* **6,** 253–268 (2004).
20. Cimini, D., Wan, X., Hirel, C. B. & Salmon, E. D. Aurora kinase promotes turnover of kinetochore microtubules to reduce chromosome segregation errors. *Curr. Biol.* **16,** 1711–1718 (2006).
21. Pinsky, B. A., Kung, C., Shokat, K. M. & Biggins, S. The Ipl1–Aurora protein kinase activates the spindle checkpoint by creating unattached kinetochores. *Nature Cell Biol.* **8,** 78–83 (2006).
22. Dogterom, M. & Yurke, B. Measurement of the force-velocity relation for growing microtubules. *Science* **278,** 856–860 (1997).
23. Janson, M. E., de Dood, M. E. & Dogterom, M. Dynamic instability of microtubules is regulated by force. *J. Cell Biol.* **161,** 1029–1034 (2003).
24. Grishchuk, E. L., Molodtsov, M. I., Ataullakhanov, F. I. & McIntosh, J. R. Force production by disassembling microtubules. *Nature* **438,** 384–388 (2005).
25. Waters, J. C., Skibbens, R. V. & Salmon, E. D. Oscillating mitotic newt lung cell kinetochores are, on average, under tension and rarely push. *J. Cell Sci.* **109,** 2823–31 (1996).
26. Westermann, S. *et al*. The Dam1 kinetochore ring complex moves processively on depolymerizing microtubule ends. *Nature* **440,** 565–569 (2006).
27. Belmont, L. D., Hyman, A. A., Sawin, K. E. & Mitchison, T. J. Real-time visualization of cell cycle-dependent changes in microtubule dynamics in cytoplasmic extracts. *Cell* **62,** 579–589 (1990).
28. Kinoshita, K., Arnal, I., Desai, A., Drechsel, D. N. & Hyman, A. A. Reconstitution of physiological microtubule dynamics using purified components. *Science* **294,** 1340–1343 (2001).
29. Verde, F., Dogterom, M., Stelzer, E., Karsenti, E. & Leibler, S. Control of microtubule dynamics and length by cyclin A- and cyclin B-dependent kinases in *Xenopus* egg extracts. *J. Cell Biol.* **118,** 1097–1108 (1992).
30. Rieder, C. L., Davison, E. A., Jensen, L. C., Cassimeris, L. & Salmon, E. D. Oscillatory movements of monooriented chromosomes and their position relative to the spindle pole result from the ejection properties of the aster and half-spindle. *J. Cell Biol.* **103,** 581–591 (1986).
31. Joglekar, A. P. & Hunt, A. J. A simple, mechanistic model for directional instability during mitotic chromosome movements. *Biophys J.* **83,** 42–58 (2002).
32. Pearson, C. G. *et al*. Stable kinetochore-microtubule attachment constrains centromere positioning in metaphase. *Curr. Biol.* **14,** 1962–1967 (2004).
33. Janson, M. E. & Dogterom, M. Scaling of microtubule force-velocity curves obtained at different tubulin concentrations. *Phys. Rev. Lett.* **92,** 248101 (2004).
34. Mandelkow, E. M., Mandelkow, E. & Milligan, R. A. Microtubule dynamics and microtubule caps: a time-resolved cryo-electron microscopy study. *J. Cell Biol.* **114,** 977–991 (1991).

1A.

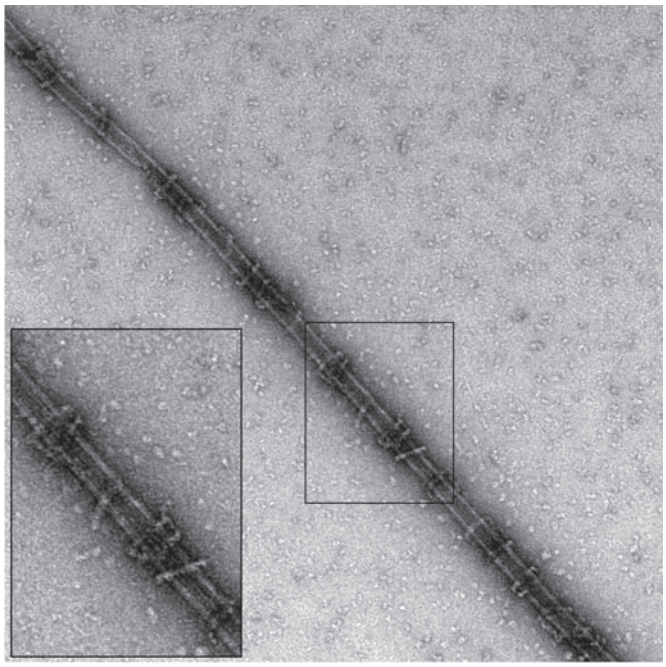

1B.

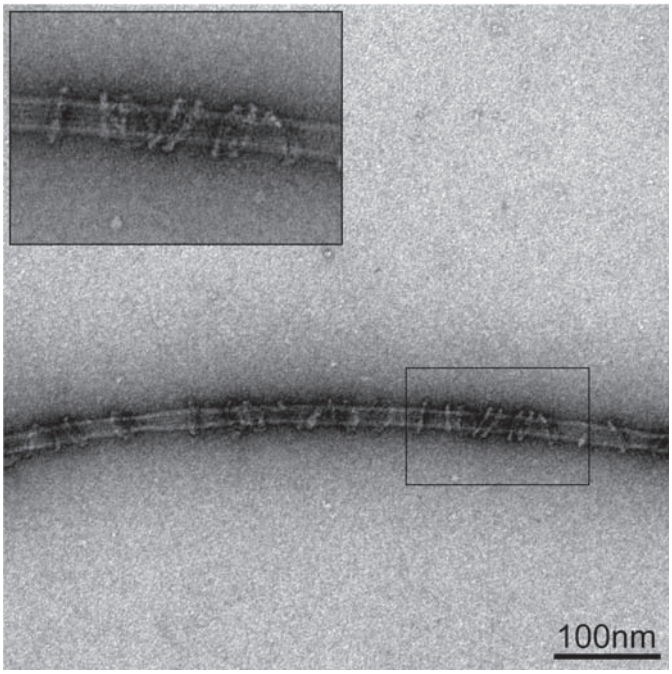

Figure S1 Electron microscopy of negatively stained preparations confirms that free Dam1 complex forms rings encircling MTs under the conditions of our *in vitro* motility experiments. (**a**) A taxol-stabilized MT decorated with 20 nM Dam1 complex in motility buffer (BRB80 supplemented with 8 mg ml^{-1} BSA, 1 mM GTP, 1 mM DTT, and an oxygen scavenging system consisting of 250 µg ml^{-1} glucose oxidase, 30 µg ml^{-1} catalase, and 4.5 mg ml^{-1} glucose). Rings encircling the MT are clearly visible. The high concentration of BSA is apparent in the background in the form of small particles. (**b**) A taxol-stabilized MT decorated with 20 nM Dam1 complex in motility buffer without BSA. Note the cleaner background.

SUPPLEMENTARY MOVIES

Movie 1 Microtubule growth, catastrophe, and shortening under tension applied through a Dam1-coated bead. The bead remains stationary in the optical trap and as the microtubule lengthens, the specimen stage moves leftward under feedback control to maintain a fixed amount of tension (here, 0.5 pN). After catastrophe, the microtubule shortens and the stage moves rightward. Bumps on the coverslip surface serve as fiducial marks showing the stage movement. The movie covers ~22 min, at 35x speed. Scale bar, 5 µm.

Movie 2 Microtubule shortening, rescue, and resumed growth under tension. The bead remains stationary in the optical trap. As the microtubule lengthens, the specimen stage moves leftward to maintain a fixed amount of tension (here, 2 pN). After catastrophe, the microtubule shortens and the stage moves rightward. After rescue, the microtubule resumes growth and the stage moves leftward. The moving cross marks a bump on the coverslip, which serves as a fiducial reference for stage movement. The fixed arrowheads mark the locations of the fiducial at an arbitrary time during growth (green arrow), at the moment of catastrophe (arrow *C*), and at the moment of rescue (arrow *R*). The movie covers ~3 min, at 5x speed. Scale bar, 5 µm.